Table V. Molecular Geometry of the 1,12-$XYB_{10}H_{11}$ Molecules so Far Studied by Gas-Electron Diffraction[a]

parameter	X = C-H Y = C	X = P Y = C	X = As Y = C	X = S Y = B
r_X	0.77	1.10	1.21	1.03
$r_X + r_B$	1.62	1.95	2.06	1.88
r(B-X)	1.710 (11)	2.052 (7)	2.137 (3)	2.010 (5)
$r(B_2-B_3)$	1.792 (7)	1.862 (16)	1.886 (6)	1.905 (4)
$r(B_3-B_7)$	1.772 (13)	1.773 (29)	1.778 (11)	1.783 (8)
$r(B_7-B_8)$	1.792 (7)	1.796 (23)	1.785 (11)	1.780 (11)
$r(B_7-Y_{12})$	1.710 (11)	1.709 (24)	1.708 (14)	1.777 (6)
ref	13	27	27	b

[a] For $B_{12}H_{12}^{2-}$, r(B-B) = 1.77 Å as determined by X-ray diffraction technique.[30] In reality there are 6 B-B bonds of 1.755 Å and 24 B-B bonds of 1.78 Å, giving the mean value of 1.77 Å; this is ascribed to specific steric interactions of hydrogen atoms and cations (K^+) in the crystal packing. r_B and r_X are taken from ref 31. [b] Present work.

various levels as well.[20c] The three kinds of computed B-H distances differ only by less than 0.01 Å. Consequently, inclusion of some ΔBH constraints would not be expected to improve the agreement.

The largest discrepancy in the geometric parameters is found for the S-B-H bond angle [3-21G(*), 110.5°; GED, 120.3°]. However, the experimental value is strongly influenced by the starting values of some vibrational amplitudes and thus is rather uncertain.

We also performed IGLO ^{11}B chemical shifts calculations employing both theoretical [3-21G(*)] and experimental (GED) structures. The $\delta(^{11}B)$ values computed for both geometries are virtually identical and are qualitatively in accord with the experimentally known chemical shifts (see Table IV). The largest discrepancy between the theoretical and experimental $\delta(^{11}B)$ values, ca. 7 ppm, is found for boron atoms B_{2-6} adjacent to sulfur. A better description of these borons, however, would require a larger basis set on sulfur for which the DZ basis is probably not sufficient.[28]

A shift to high frequency of B_{12} ($\delta(^{11}B)$ = 19.2 ppm) with respect to the "parent" $B_{12}H_{12}^{2-}$ is well reproduced by the calculations (IGLO DZ: 24.5 ppm). A more detailed discussion of this "antipodal effect"[32] will be published elsewhere.

Note Added in Proof. We were not aware of the 6-31G* geometry[22] when the present contribution had gone to press. The results are as follows (in Å): r(S-B), 2.018; $r(B_2-B_3)$, 1.904; $r(B_3-B_7)$, 1.771; $r(B_7-B_8)$, 1.804; $r(B_7-B_{12})$, 1.794; $r(B_2-H_{13})$, 1.177; $r(B_7-H_{18})$ and $r(B_{12}-H_{23})$, 1.182. There is an excellent agreement of the first two parameters with the corresponding GED ones. The IGLO values (DZ//6-31G*, in ppm) are (B_{2-6}) -0.7, (B_{7-11}) -10.0, and (B_{12}) 23.1 ppm, quite similar to the DZ//GED and DZ//3-21G(*) results.

Acknowledgment. We thank Mrs. M. Kolonits for experimental work and Professor I. Hargittai for his interest and valuable comments. Financial support from the Hungarian National Scientific Research foundation (OTKA No. 132) is gratefully acknowledged. D.H. expresses a gratitude to the members of the Budapest group for their hospitality during his stay in Budapest in 1990. We also thank Professor W. Kutzelnigg, Dr. M. Schindler, and Mr. U. Fleischer for the IGLO program. M.B. acknowledges a grant from the Studienstiftung des Deutschen Volkes. Stimulating discussion with Dr. J. D. Kennedy are highly appreciated as well.

Registry No. 1-$SB_{11}H_{11}$, 56464-75-6.

Supplementary Material Available: Listings of total electron diffraction intensities for both camera distances (2 pages). Ordering information is given on any current masthead page.

(28) Schindler, M. *J. Chem. Phys.* **1988**, *88*, 7638.

(29) The estimated total errors for distances are $\sigma_t = [(0.002r)^2 + 2\sigma^2 + (\Delta/2)^2]^{1/2}$, for angles $\sigma_t = [2\sigma^2 + (\Delta/2)^2 + (\Delta_1/2)^2]^{1/2}$, where 0.002 means experimental scale error, σ is the standard deviation from the least-squares refinement (see Tables I and II) multiplied by $\sqrt{2}$ to take the consequences of data correlation into account, and Δ is the maximum difference in the four sets of results A-D. Δ_1 is the difference between the values of the bond angles obtained for the model A, where l(B···H)[e] (see Table I) and l(S···H_{13}) were refined to 0.100 and 0.130 Å, respectively, and for such model, where these amplitudes were refined to 0.123 and 0.153 Å, respectively.

(30) Wunderlich, J. A.; Lipscomb, W. N. *J. Am. Chem. Soc.* **1960**, *82*, 4427.

(31) Vilkov, L. V.; Mastryukov, V. S.; Sadova, N. S. *Determination of the Geometrical Structure of Free Molecules*; Mir Publishers: Moscow, 1983.

(32) See, e.g.: Heřmánek, S.; Hnyk, D.; Havlas, Z. *J. Chem. Soc., Chem. Commun.* **1989**, 1859 and references therein.

Contribution from the Istituto di Chimica Strutturistica Inorganica, Via Venezian 21, 20133 Milano, Italy

Transition Metal Carbonyl Clusters. A Molecular Mechanics Approach to Ligand Stereochemistry

Angelo Sironi

Received August 22, 1991

The surface force field for molecular mechanics simulation of the ligand structure in transition metal carbonyl clusters, originally developed by Lauher, is redesigned and implemented in the common MM2 Allinger's program. The equal potential surface (EPS) for a cluster is built by patchwork using patches whose shape depends on Crabtree and Lavin's reaction path for the terminal/μ_2-bridging/terminal interconversion. The CO ligands can float on the EPS even in the presence of a clear connectivity pattern (necessary for the energy minimization within the MM2 scheme) because their connectivity is periodically redetermined. *A CO ligand is assumed to be locally connected to the metals used to generate the patches to which the ligand belongs.* The program is a powerful modeler and can be used as a *source of sterically reasonable geometries.* The dominant contribution to the computed steric energies arises from the nonbonded interactions; hence, the comparison of modeled and experimental structures should lead to the recognition of other forces at work. Consideration is given to the case of octahedral metal carbonyl clusters with stoichiometries ranging from $M_6(CO)_{12}$ to $M_6(CO)_{20}$, and since "real" structures are only occasionally found in the global minimum of the "steric" potential energy surface, *it would appear that intramolecular steric interactions are not the leading term in determining the metal carbonyl cluster stereogeometries in the solid state.* It is only the interplay between many different factors (inter- and intramolecular steric interactions, charge and local bookkeeping equilization, and more specific electronic effects) that determines the real structure. *Steric energies are properly used only to justify small distortions around a given geometry or to exclude a particularly crowded stereoisomer rather than to foresee the correct one.*

The cornerstone of all rationale concerning carbonyl clusters[1-4] is the assumption that the number of ligands and their stereochemistry do not affect the overall number of cluster valence electrons (CVEs), the only relevant factor being the metal cluster

0020-1669/92/1331-2467$03.00/0

geometry. There are systematic and individual exceptions,[5] but one confirmation comes from the isoelectronicity of the octahedral clusters which, in order to fulfil the 86-CVE requirement, display a variety of ligand stereochemistries, ranging from the carbonyl-to-metal ratio (CMR) of 12/6 in $[Ni_6(CO)_{12}]^{2-}$[6] to that of 19/6 in $[Re_6C(CO)_{19}]^{2-}$.[7]

Many observations concur to suggest that the ligand stereochemistry depends on small, cooperative or not, interactions and that the potential energy surface (PES) of the metal carbonyl cluster is quite soft with respect to ligand mobility. For instance, in a few cases two isomers of the same metal carbonyl cluster, differing only in the ligand disposition, have been structurally characterized in the solid state: $Ir_6(CO)_{16}$,[8] $[Ru_6C(CO)_{16}]^{2-}$,[9] $H_3Ru_4(CO)_{13}$,[10] and $[Rh_{11}(CO)_{23}]^{3-}$.[11] Moreover, the stereochemical nonrigidity, as well as the presence in solution of two or more isomers, is well documented for many metal clusters.[12] Even if there is no general theory for rationalizing the overall observed behavior, carbonyl mobility around the cluster surface has always been related to the carbonyl's ability to act as a two-electron donor whenever carbon is the only donor atom. Indeed, the variety of their bonding capabilities and the multitude of cluster orbitals available for metal–metal and metal–ligand bonding allow the stabilization of conceivable transition states and the lowering of the fluxionality barriers. The behavior of carbon monoxide coordination has been exhaustively reviewed by Horwitz and Shriver.[13] A "reaction" trajectory for terminal/μ_2-bridge/terminal carbonyl exchange between two iron atoms was recently obtained by Crabtree and Lavin,[14] using the structure correlation method,[15] demonstrating the earlier Cotton suggestion that there is a smooth continuum which encompasses terminal, bent semibridging, and symmetrically bridging CO groups.[16]

After the appearance in the 1960s of the first structurally characterized binary carbonyl metal clusters (BCMCs), two factors were soon recognized as driving the ligand stereochemistry: (i) favorable packing of the CO ligands about the cluster core;[17] (ii) charge equalization over all the metal atoms.[16,18,19] Point i was qualitatively,[20] and later quantitatively,[21] investigated by Johnson et al., who searched for the best fit between the metal cluster and the optimum ligand polyhedron, determined using a "point on a sphere" repulsion model. More recently, Lauher[22] extensively studied the stereochemistry of BCMCs with, at most, four metal atoms, using a molecular mechanics (MM) approach, which has inspired this contribution and which will be discussed in detail in the following sections.

Inorganic Molecular Mechanics

The first MM study of a metal complex was reported as early as 30 years ago,[23] but inorganic chemistry has still to see the explosion of interest that this technique stimulated in the organic field, where it has been successfully applied to many problems.[24] The majority of the inorganic studies have concerned cobalt(III) amine complexes,[25] but recently other systems have been tackled: polynuclear complexes with high-order metal–metal bonds,[26] crown ether alkaline-earth-metal complexes,[27] transition-metal π-complexes,[28] square-planar transition-metal complexes,[29] and metal clusters.[22,30,31]

The main problem is that reliable estimates of the deformation force constants for bonding parameters involving the metal are difficult to obtain. In fact, metal centers not only display a larger stereochemical variability (thus requiring a wider number of parameters) but are also theoretically and experimentally less studied than the corresponding organic building blocks, which are simpler, accessible to quantum mechanical computations, and structurally and spectroscopically well characterized.

The limited number of observations to fit during the parametrization procedure imposes a series of more or less arbitrary decisions, possibly resulting in an intrinsic weakness of the derived force field. Moreover, moving from the tetrahedral (CR_4) to the octahedral (ML_6) coordination (the most common in inorganic systems), bending (and torsional) parameters do not depend on the involved atom types only; they are also position dependent. That is, while the R–C–R angles are all equivalent (therefore possessing a unique reference value), the L–M–L_{cis} and the L–M–L_{trans} angles are not, requiring multiple reference values (a new approach to the problem has recently been reported).[29] The problem becomes even more complicated when other stereochemistries and coordination numbers are considered. Therefore, there is no single way to deal with metal atoms, and different systems have to be treated with different ad hoc assumptions. Whenever the metal atom environment is well defined, it is convenient to describe the angular reference values exactly, but as far as stereochemical flexibility at the metal center is concerned, it is convenient to avoid any assumption regarding the L–M–L (and torsional) angles and to consider explicitly the 1,3 nonbonded interactions.[32] The latter approach clearly excludes any electronic contribution to the metal atom stereochemistry; nevertheless, it

(1) (a) Mingos, D. M. P. *Nature* **1972**, *236*, 99. (b) Mingos, D. M. P. *Acc. Chem. Res.* **1984**, *17*, 311. (c) Mingos, D. M. P.; Johnston, R. L. *Struct. Bonding* **1987**, *68*, 29.

(2) (a) Wade, K. *Chem. Br.* **1975**, *11*, 177. (b) Wade, K. *Adv. Inorg. Chem. Radiochem.* **1976**, *18*, 1.

(3) (a) Teo, B. K. *Inorg. Chem.* **1984**, *23*, 1251. (b) Teo, B. K.; Longoni, G.; Chung, F. R. K. *Inorg. Chem.* **1984**, *23*, 1257.

(4) Lauher, J. W. *J. Am. Chem. Soc.* **1978**, *100*, 5305.

(5) Triangular platinum clusters usually have less than the 48 CVEs expected. The octahedral $Ni_6(C_5H_5)_6$ cluster has 90 rather than 86 CVEs. $Rh_{12}H_2(CO)_{25}$ (Ciani, G.; Sironi, A.; Martinengo, S. *J. Chem. Soc., Chem. Commun.* **1985**, 1557) and $[Ir_{12}(CO)_{26}]^{2-}$ (Della Pergola, R.; Demartin, F.; Garlaschelli, L.; Manassero, M.; Martinengo, S.; Sansoni, M. *Inorg. Chem.* **1987**, *26*, 3487) have similar metal clusters but different electron counts.

(6) Calabrese, J. C.; Dahl, L. F.; Cavalieri, A.; Chini, P.; Longoni, G.; Martinengo, S. *J. Am. Chem. Soc.* **1974**, *96*, 2616.

(7) Beringhelli, T.; D'Alfonso, G.; Molinari, H.; Sironi, A. *J. Chem. Soc., Dalton Trans.* **1992**, 689.

(8) Garlaschelli, L.; Martinengo, S.; Bellon, P. L.; Demartin, F.; Manassero, M.; Chiang, M. Y.; Wei, C.; Bau, R. *J. Am. Chem. Soc.* **1984**, *106*, 6664.

(9) C_{2v}-$[AsPh_4]^+$ salt: Johnson, B. F. G.; Lewis, J.; Sankey, S. W.; Wong, K.; McPartlin, M.; Nelson, W. J. H. *J. Organomet. Chem.* **1980**, *191*, C3. C_s-$[NEt_4]^+$ salt: Bradley, J. S.; Ansell, G. B.; Hill, E. W. *J. Organomet. Chem.* **1980**, *184*, C33. Ansell, G. B.; Bradley, J. S. *Acta Crystallogr.* **1980**, *B36*, 726.

(10) McPartlin, M.; Nelson, W. J. H. *J. Chem. Soc., Dalton Trans.* **1986**, 1557 and references therein.

(11) Fumagalli, A.; Martinengo, S.; Ciani, G.; Sironi, A.; Heaton, B. T. *J. Chem. Soc., Dalton Trans.* **1988**, 163.

(12) Johnson, B. F. G.; Benfield, R. E. In *Transition Metal Clusters*; Johnson, B. F. G., Ed.; Wiley: New York, 1980; p 471.

(13) Horwitz, C. P.; Shriver, D. F. *Adv. Organomet. Chem.* **1984**, *23*, 219.

(14) Crabtree, R. H.; Lavin, M. *Inorg. Chem.* **1986**, *25*, 805.

(15) Bürgi, H. B.; Dunitz, J. D. *Acc. Chem. Res.* **1983**, *16*, 153.

(16) Cotton, F. A. *Prog. Inorg. Chem.* **1976**, *21*, 1.

(17) Wei, C. H.; Dahl, L. F. *J. Am. Chem. Soc.* **1969**, *91*, 1351.

(18) Churchill, M. R.; Veidis, M. V. *J. Chem. Soc. A* **1971**, 2170; 2995.

(19) Cotton, F. A.; Troup, J. M. *J. Am. Chem. Soc.* **1974**, *96*, 1233.

(20) Johnson, B. F. G. *J. Chem. Soc., Chem. Commun.* **1976**, 211.

(21) (a) Benfield, R. E.; Johnson, B. F. G. *J. Chem. Soc., Dalton Trans.* **1980**, 1743. (b) Johnson, B. F. G.; Benfield, R. E. *Top. Stereochem.* **1981**, *12*, 253.

(22) Lauher, J. W. *J. Am. Chem. Soc.* **1986**, *108*, 1521.

(23) Corey, E. J.; Bailar, J. C. *J. Am. Chem. Soc.* **1959**, *81*, 2620.

(24) See for example: Burkert, U.; Allinger, N. L. *Molecular Mechanics*; ACS Monograph 177; American Chemical Society: Washington, DC, 1982.

(25) Brubaker, G. R.; Johnson, D. W. *Coord. Chem. Rev.* **1984**, *53*, 1.

(26) Boeyens, J. C. A. *Inorg. Chem.* **1985**, *24*, 4149.

(27) Burns, J. H.; Kessler, R. M. *Inorg. Chem.* **1987**, *26*, 1370.

(28) Slovokhotov, Y. L.; Timofeeva, T. V.; Struchkov, Y. T. *Zh. Strukt. Khim.* **1987**, *28*, 3.

(29) Allured, V. S.; Kelley, C. M.; Landis, C. R. *J. Am. Chem. Soc.* **1991**, *113*, 1.

(30) Clare, B. W.; Favas, M. C.; Kepert, D. L.; May, A. S. In *Advances in Dynamic Stereochemistry*; Gielen, M. F., Ed.; Freund Publishing House Ltd.: London, 1985; p 1.

(31) Horwitz, C. P.; Holt, E. M.; Shriver, D. F. *Inorg. Chem.* **1984**, *23*, 2491.

(32) (a) Hambley, T. W.; Hawkins, C. J.; Palmer, J. A.; Snow, M. R. *Aust. J. Chem.* **1981**, *34*, 45. (b) Ferguson, D. M.; Raber, D. J. *J. Comput. Chem.* **1990**, *11*, 1061.

is always possible to add some specific "electronic effect" by constraining a few bond angles.

As beautifully outlined by Lauher,[22] a MM treatment of BCMCs requires the introduction of the equal potential surface (EPS) concept (which was nevertheless anticipated in ref 30) to catch all the bonding modes of the carbonyl ligands. A clear-cut distinction between the carbonyl ligand coordination modes is, in fact, missing and a terminal CO can smoothly transform into a μ_2- or μ_3-bridging carbonyl.[13,14] To describe in a unified way all the intermediate conformations of the concerted motion of some of the CO ligands about the metal frame (carbonyl scrambling), where the individual metal–carbon connectivity is not conserved, it is convenient to assume a global carbonyl-to-cluster connectivity (which is indeed conserved). In other words, the CO ligands are envisaged as if they were bonded to the metallic cluster as a whole, their carbon atoms being free to float on the EPS, maintaining the C–O vector normal to the surface. In spite of the simplicity of this idea, its inclusion in a preexistent MM program is a rather complex task because the atom–atom connectivity is a central assumption of all the MM computations.[33]

To bypass these problems, it was decided to follow a slightly different approach by considering the CO ligands to be only "Locally connected", i.e. periodically redetermining their connectivity on the basis of their actual coordinates until convergence. This required a different, more flexible, EPS definition (vide infra) but eventually resulted in the implementation of the EPS algorithm in Allinger's MM2 program with full retention of all its features.[34] The metal framework can thus be optimized together with the ligand geometry, symmetry constraints can be imposed, and the cluster stereochemistry can be straightforwardly studied in the presence of other "organic" ligands. The basic idea of redetermining some of the parameters (in the present case, the connectivity) on the basis of the actual geometry is not foreign to MM: the torsional constants around conjugated double bonds are, for instance, redetermined after each convergence phase in the MMP2 version of MM2.[34]

Analytical Description of the Carbonyl Exchange Trajectories

In the present approach, the three-dimensional shape of the EPS will be derived as a function of the observed metal covalent radius (R_m) and metal–carbon interactions (R_t, R_{μ_2}, and R_{μ_3} are the reference M–C$_t$, M–C$_{\mu_2}$, and M–C$_{\mu_3}$ bond distances, respectively), from the experimental knowledge of the (two-dimensional) reaction path for the terminal/μ_2-bridging/terminal (t/μ_2/t) interconversion,[14] which, for computational purposes, must be described analytically. An analytical description of the terminal/μ_3-bridging/μ_2-bridging (t/μ_3/μ_2) interconversion is also needed.

A reasonable description of the t/μ_2 carbon atom path is shown in eq 1, obtained by joining a circle (of radius R_t) to an exponential

$$y = (R_t^2 - x^2)^{1/2} \qquad 0 \le x \le J_x \tag{1a}$$

$$y = H_{\mu_2} + A \exp(-Bx/(C - x)) \qquad J_x < x \le R_m \tag{1b}$$

function (such that at $x = R_m$ the computed M–C distance is equal to R_{μ_2}) at ($J_x = R_t \cos 75°$, $J_y = R_t \sin 75°$). In eq 1, $H_{\mu_2} = y(R_m) = (R_{\mu_2}^2 - R_m^2)^{1/2}$ is the height of the carbon atom above the middle of the spanned edge, while $C = 1.1R_m$, $B = J_x(C - J_x)^2/(CJ_y(J_y - H_{\mu_2}))$, and $A = (J_y - H_{\mu_2})/\exp(-BJ_x/(C - J_x))$ have been derived from the boundary condition imposing the continuity of the function and its first derivative at the junction point. The full t/μ_2/t reaction path is then obtained by joining a t/μ_2 to a μ_2/t pathway. In the more general case, the two metal centers can be described by two different parameter sets (a and b) and the t/μ_2/t path will not be symmetric, but because it must be continuous ($H_{\mu_2}^{a} = H_{\mu_2}^{b}$), not all the parameters of the two sets are independent. A comparison with the experimental values of Crabtree and Lavin[14] is reported in Figure 1.

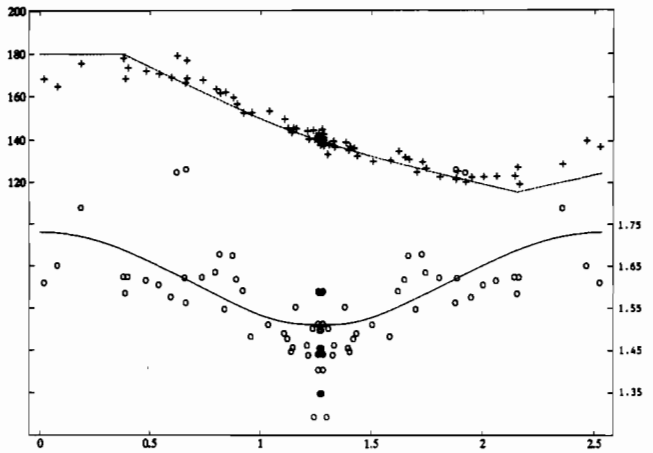

Figure 1. Reaction path for the t/μ_2/t process studied by Crabtree and Lavin.[14] Data have been taken from ref 14 (iron derivatives only) after normalization to a Fe–Fe bond distance of 2.535 Å: (O) experimental carbon atom coordinates; (+) experimental M–C–O angles. The full line is the C atom path described by eq 1 when $R_t = 1.73$, $R_{\mu_2} = 1.972$, and $R_m = 1.267$ Å. The dashed line is the M–C–O path derived from the linear relation between Ψ (the M–M–C angle) and θ (the M–C–O angle) observed by Crabtree and Lavin.[14] Note that the hypothesis that the C–O vector has to be perpendicular to the C atom path is not consistent with the above relation (see Figure 3).

By analogy with the t/μ_2 case, the t/μ_3 reaction path can be reasonably described by substituting in eq 1 (and in *A*, *B*, and *C*) R_m, R_{μ_2}, and H_{μ_2} with R_c ($=2 \times 3^{-1/2}R_m$), R_{μ_3}, and H_{μ_3} ($=y(R_c) = (R_{\mu_3}^2 - R_c^2)^{1/2}$), respectively. The full t/μ_3/μ_2 reaction path is then completed by adding a cosine function to account for the μ_3/μ_2 path ($R_e = 3^{1/2}R_m$):

$$y = (R_t^2 - x^2)^{1/2} \qquad 0 \le x \le J_x \tag{2a}$$

$$y = H_{\mu_3} + A \exp(-Bx/(C - x)) \qquad J_x < x \le R_c \tag{2b}$$

$$y = 0.5((H_{\mu_2} + H_{\mu_3}) + (H_{\mu_2} - H_{\mu_3}) \cos(2\pi(x - R_c)/(R_e - R_c))) \qquad R_c \le x \le R_e \tag{2c}$$

Such a description of the t/μ_3/μ_2 pathway strictly refers only to a carbonyl ligand bridging an equilateral face. Nevertheless, as in the t/μ_2/t case, the metals can be described by three different parameter sets (a, b, and c), provided that they are properly chosen to ensure the continuity of the paths ($H_{\mu_2}^{a} = H_{\mu_2}^{b} = H_{\mu_2}^{c}$ and $H_{\mu_3}^{a} = H_{\mu_3}^{b} = H_{\mu_3}^{c}$). Of course, in such a case, the reference triangle will be scalene and the reported relationships among R_m, R_c, and R_e no longer valid. Hence the "real" R_c and R_e values must be determined on the basis of the actual triangle shape to derive the proper pathways.

Equal Potential Surface—a Redesign

Lauher faced the problem of modeling an EPS for carbonyl clusters by using the formalism Connolly developed in his computations of the solvent-excluded molecular volume.[35] Lauher's EPS is the "solvent-accessible surface" of the naked metal cluster, i.e. "the smooth network of convex and reentrant surfaces traced by the inward-facing part of a probe sphere as it rolls over the molecule".[35] Its shape depends primarily on two quantities: (i) the radius of the spheres modeling the metal atoms (set to be equal to the M–C(terminal) bond distance); (ii) that of the probing sphere (adjusted in order to obtain reasonable M–C(bridging) bond distances).

In the present approach, the three-dimensional shape of the EPS is extrapolated from the bidimensional t/μ_2/t and t/μ_3/μ_2 reaction paths of the carbonyl ligands, described analytically by eqs 1 and 2. In practice, the EPS is derived by the following assumptions: (i) in the case of a mononuclear complex (like $Cr(CO)_6$), the EPS is assumed to be a sphere of radius R_t; (ii) in the case of a dimer (like $Fe_2(CO)_9$), the peanut-shaped EPS is assumed to be the

(33) Lauher has developed a rather unsophisticated program which alternates direct search with Newton–Raphson energy minimization and constrains the metal framework to rigidity.

(34) Allinger, N. L.; Yuh, Y. H. QCPE Program No. 395.

(35) Connolly, M. L. *J. Am. Chem. Soc.* **1985**, *107*, 1118.

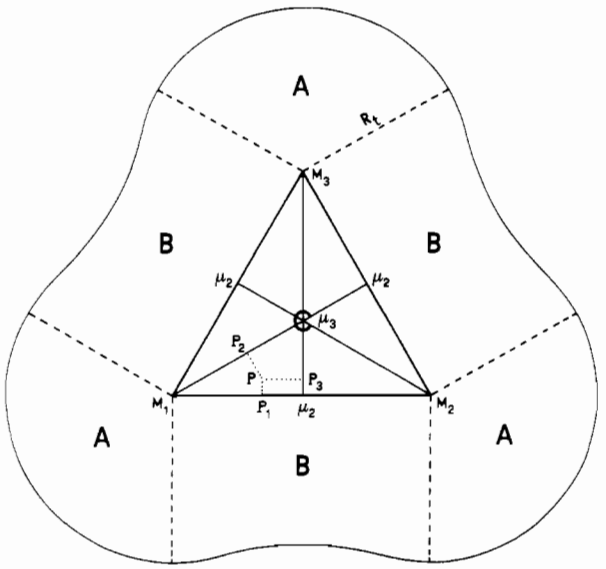

Figure 2. Partition of the plane of a triangular cluster using lines orthogonal to the edges (dashed). The curved envelope traces the EPS in the plane. *P* is the projection of the carbon atom in the metal plane. The EPS is determined as follows: (a) when *P* belongs to the A region, the carbonyl ligand is under the influence of a single metal center (the leading vertex) and the EPS is assumed to be a (part of a) sphere of radius R_t; (b) when *P* belongs to the B region, the carbonyl ligand is under the influence of two metal centers (the leading edge) and the EPS is assumed to be the turned surface generated by eq 1; (c) when *P* belongs to the C region, the carbonyl ligand is under the influence of three metal centers (the leading face) and the EPS is determined by interpolation. The elevation of the EPS, above or below *P*, will be the mean (weighted by the reciprocal of the P–P_1, P–P_2, and P–P_3 distances) of those computed in P_1, P_2, and P_3 on the basis of eqs 1 (P_1) and 2 (P_2 and P_3). In the case of mixed-metal clusters, the triangle is no longer equilateral, the μ_2 points no longer bisect the edges, and the μ_3 point is somewhere in the middle of the triangle; nevertheless, the same procedure applies because the three M_i–μ_2 vectors still share a common point μ_3 (note that P–P_1 is chosen to be parallel to the μ_3–μ_2 vector, which is not necessarily orthogonal to the edge).

turned surface generated by eq 1 (plus one spherical cup on each end); (iii) in the case of a triangular cluster (like $Fe_3(CO)_{12}$), the EPS shape will depend on both the t/μ_2/t (eq 1) and the t/μ_3/μ_2 (eq 2) reaction paths, its elevation above or below the triangle being computed with the procedure described in the caption to Figure 2; (iv) in the case of a convex cluster, the EPS is assumed to be a complex surface obtained by patchwork using the above defined spherical, cylindrical, and triangular patches whose particular shape ensures continuity and smoothness of the whole surface; (v) square and larger polygonal faces have an EPS generated by the edges only; (vi) concave butterfly cavities supporting η^2-μ_3-CO[36] or η^1-μ_4-CO[37] are usually beyond the scope of the present approach.

In the original formulation, the EPS term stood for the surface where the CO ligands were free to move about, without suffering any "metal-determined" potential energy change, as long as the C atom and the C–O vector were respectively kept tied and perpendicular to the surface. Nevertheless, the two-dimensional implication of the latter hypothesis (i.e., the C–O vector has to be perpendicular to the t/μ_2/t carbon atom path) is inconsistent with the experimental finding of a linear relationship between the M–M–C and the M–C–O angles (see Figure 3).[14] Thus, even if the C–O vectors cannot be really far from being perpendicular to the EPS, the "natural" M–C–O angles are computed by assuming the linear relationship between the M–M–C and the M–C–O angles. The probe sphere method is more general because it can be applied to clusters of any geometry, while the patchwork method has still to be extended to concave clusters. Nevertheless,

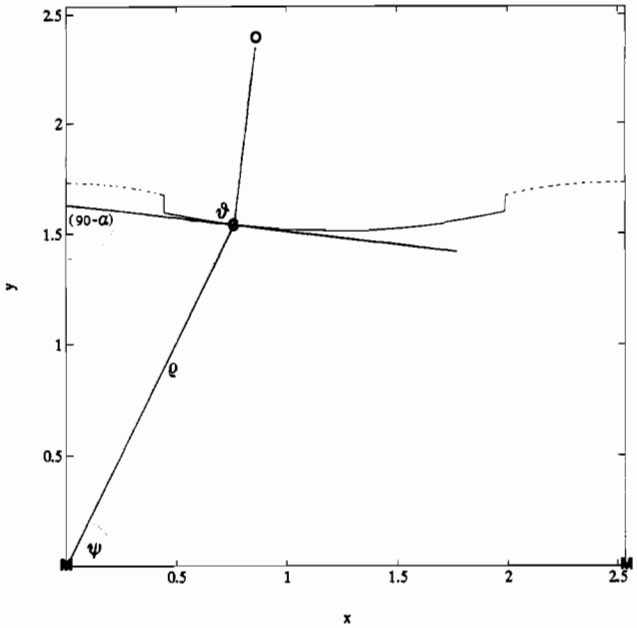

Figure 3. Reaction path for the t/μ_2/t process as obtained from the following assumptions: (i) the C–O vector is perpendicular to the C atom path ($\alpha = \theta - \Psi - 90°$); (ii) M–M–C ($\Psi$) and M–C–O ($\theta$) are linearly related ($\theta = B\Psi + \omega$) for $\Psi < 75°$; (iii) Ψ and θ are uncorrelated when $\Psi > 75°$. *The fact that it is not continuous implies that the three hypotheses cannot be simultaneously true.* The continuous line is the plot of the function $\rho = k[\sin(B\Psi) - \cot\omega\cos(B\Psi)]^{-1/B}$ for $\Psi < 75°$, which is the solution of the following differential equation (settled from (i) and (ii)): (in Cartesian coordinates) $dy/dx = \tan\alpha = \cot((B-1)\Psi - \omega)$; (in polar coordinates) $[(d\rho/d\Psi)\sin\Psi + \rho\cos\Psi]/[(d\rho/d\Psi)\cos\Psi - \rho\sin\Psi] = \cot((B-1)\Psi - \omega)$. The integration constant k is determined from the boundary condition $\rho = R_{\mu_2}$ at $x = R_m$. The dashed lines are circles of radius R_t describing the behavior of a carbonyl ligand when $\Psi > 75°$ ($\theta = 180°$ for $\Psi > 75°$ in agreement with (iii)). If the three hypotheses were consistent, the continuous and dashed lines should merge smoothly at $\Psi = 75°$. However, for the iron compounds (R_m = 1.267, R_t = 1.73, R_{μ_2} = 1.972 Å, B = 1.51, ω = 64.5°) studied by Crabtree and Lavin,[14] and also in general (for reasonable R_m, R_t, and R_{μ_2} values), this does not happen. We must nevertheless remember that a physical explanation for point (ii) is lacking and that other functions would appear to fit the Crabtree and Lavin data equally well. It is therefore better to consider the linear relationship only as a useful tool for devising a "reasonable" M–C–O angle.

Scheme I

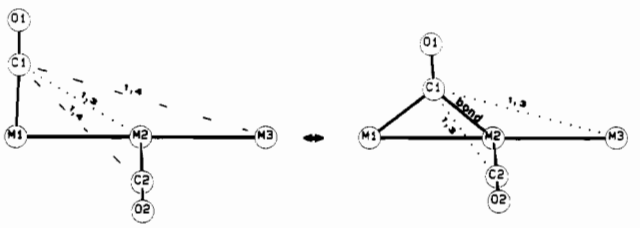

it could be considered more physically sound (because it incorporates the experimental findings about the t/μ_2/t reaction path) and the explicit use of R_{μ_2} and R_{μ_3} as parameters makes the final stereogeometry more precisely addressable (this could be significant when the program is used as a molecular builder). However, the resulting EPSs calculated from the two methods are similar and the main reason for choosing the patchwork method was that it naturally conveys the local connectivity concept, which allows the merging of the "usual" MM and the EPS formalisms.

Locally Connected Carbonyl Ligands

The procedure outlined above allows a simple definition of the carbonyl (local) connectivity because the EPS is naturally partitioned into the constituting patches. *The carbon atom will be (locally) connected to the metals (of the leading vertex, edge,*

(36) Manassero, M.; Sansoni, M.; Longoni, G. *J. Chem. Soc., Chem. Commun.* **1976**, 919.
(37) Li, P.; Curtis, M. D. *J. Am. Chem. Soc.* **1989**, *111*, 8279.

Scheme II

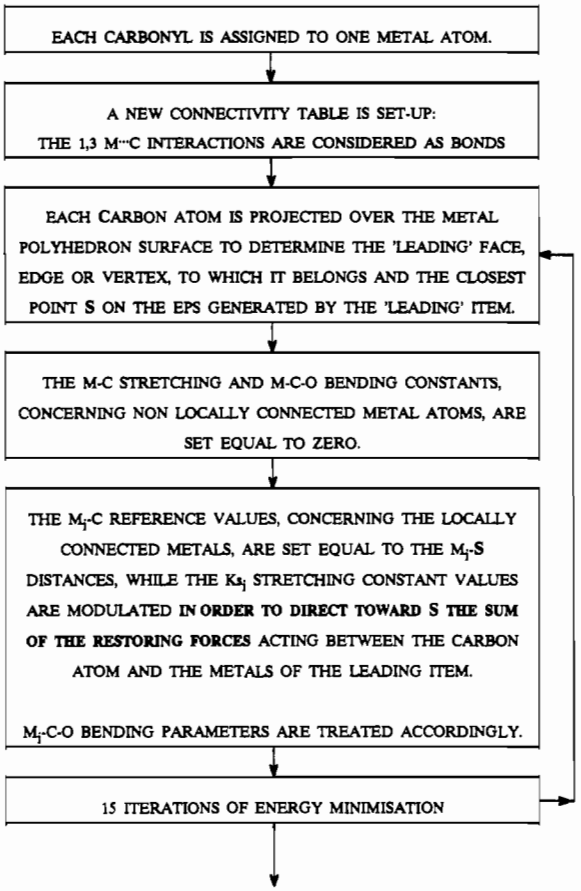

or face) used to generate the patch to which it belongs.

When the energy is minimized, a carbonyl ligand, under the influence of (mainly) the nonbonded interactions, can leave its original patch and fall under the influence of different metal atoms. Thus, the nature of the M/C and C/C interactions is variable since, as outlined in Scheme I, when a carbonyl floats over the EPS, some previous M–C bond becomes a 1,3 M···C nonbonded interaction (and vice versa) while some previous 1,3 C···C nonbonded interaction converts to a 1,4 one (and vice versa).

Bonding and nonbonding interactions are described by potential wells of different depths and shapes and, more importantly in this context, have different reference systems; i.e., the former are zero at the "natural" bond length, while the latter are zero at infinity. Thus, to ensure continuity for the energy functional over the EPS, the vdW parameters for the metal atoms must be set to zero (for a smooth interchange of the M/C bonding and nonbonding terms) and the 1,3 C···C nonbonded interactions must be considered explicitly (for a smooth 1,3/1,4 interchange), while the C–M–C bendings, together with any torsional term, must be omitted.

The Program

The starting point was Allinger's MM2 program.[34] This was modified (i) to take into account atom connectivities larger than 4 and (ii) to periodically reset the metal–carbonyl connectivity together with the M–C and M–C–O force constants and reference values. The flux diagram for the new program is shown in Scheme II.

The adopted force field parameters are reported in Table I. They are the parameters of the usual stretching, bending, and dipole–dipole interaction equations adopted in MM2. The reported M–C reference values concern terminal and symmetric bridging (μ_2 and μ_3) carbonyl ligands and are used to compute the EPS. For each minimization cycle, the *actual* M_i–C reference values (meaningful only if the metal and carbon atoms are locally connected) are the distances between the metals and the EPS point closest to the carbon atom. The restoring force between the EPS and a particular carbon atom is the vectorial sum of all the M_i–C restoring force acting between that carbon and its locally connected metal atoms. For each minimization cycle, the *actual* K_{s_i} values are shaped to fit the reported K_s value for the surface–C stretching (see Figure 4).

For the van der Waals interactions, the new MM3[38] force field was adopted, as larger but softer atoms better account for the experimental M–C–M angles which are mainly governed by a balance between the 1,4 and 1,3 nonbonded interactions when the latter are considered explicitly, as in the present approach. Moreover the MM3 force field can also be used to describe the intermolecular interaction,[38] and this might lead to the inclusion of molecular packing effects in the future.

Table I

Stretching and Bending Parameters			
K_s (surface–C)	3.0 mdyn/Å	K_b(surface–C–O)	0.5 mdyn/deg
K_s(C–O)	12.0 mdyn/Å	cubic stretch term	−2.0 mdyn/Å^2
K_s(M–M)	2.0 mdyn/Å		

Charge Interaction Parameters

CO dipole moment 0.552 D[a] dielectric constant 1.5

van der Waals Parameter

	e_{vdW}, kcal/mol	R_{vdW}, Å		e_{vdW}, kcal/mol	R_{vdW}, Å
C	0.027	2.04	O	0.031	1.87

Bond Length Parameters, Å

set	M–M	M–C_t	M–C_{μ_2}	M–C_{μ_3}	C–O
A	2.50	1.70	1.85	2.00	1.15
B	2.60	1.75	1.90	2.05	1.15
C	2.70	1.80	1.95	2.10	1.15
D	2.75	1.825	1.975	2.125	1.15
E	2.80	1.85	2.00	2.15	1.15
F	2.90	1.90	2.05	2.20	1.15
G	3.00	1.95	2.10	2.25	1.15

[a] Corresponding to a charge separation of 0.1 e at 1.15 Å.

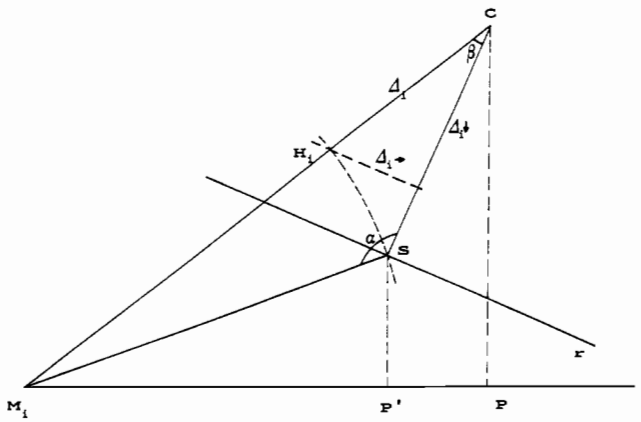

Figure 4. Shaping of the local force constants and reference values for the M_i–C interactions. This is necessary in order to direct toward the closest EPS point the sum of the restoring forces acting between the carbon atom and its locally connected metals. The plane presented in the picture is that containing a locally connected metal M_i, the C atom, and its closest EPS point S, r is the intersection line between the picture plane and the one tangent to the EPS (in S). M_i–S will be the *local* reference value for the M_i–C bond distance. The stretching force, acting on the C carbon atom, due to the M_i–C bond will be proportional to $K_{s_i}\Delta_i$ (Δ_i = C–H_i; K_{s_i} is the *local* stretching constant). $\Delta_{i\rightarrow} = \Delta_i \sin\beta$ and $\Delta_i\downarrow = \Delta_i \cos\beta$ are the tangential and orthogonal force components, respectively. In each minimization cycle the K_{s_i} values for the M_i–C interactions are computed by solving the system of the following equations: $\sum_i K_{s_i}\Delta_{i\rightarrow}{}^x = 0$, $\sum_i K_{s_i}\Delta_{i\rightarrow}{}^y = 0$, and $\sum_i K_{s_i}\Delta_i\downarrow = K_s|C–S|$, where x and y are two perpendicular directions in the plane orthogonal to the C–S vector, K_s is the C–surface stretching constant, and i applies to all locally connected (to carbon) metal atoms.

(38) Allinger, N. L.; Yuh, Y. H.; Lii, J.-H. *J. Am. Chem. Soc.* **1989**, *111*, 8551.

Table II[a]

I	$[M_6(CO)_{20}]$	31.2 ^5G (C_{3v})	
II	$[Re_6C(CO)_{19}]^{2-}$	29.6 ^5G (C_2)	24.9 ^5G (C_s)
III	$[M_6(CO)_{19}]$	27.5 ^5G (C_{3v})	25.3 ^5G (C_3)
IV	$[Ru_6H(CO)_{18}]^-$	44.7 ^5E (C_{3v})	31.2 ^5E (D_3)[m]
V	$[Ru_6(CO)_{18}]^{2-}$	34.1 ^5E (C_2)	31.9 *E (C_2)
VI	$[M_6(CO)_{18}]$	34.9 ^5E (C_2)	31.9 *E (C_2)
VII	$[Ru_6C(CO)_{17}]$	23.5 ^5E (C_2)	
VIII	$[MoFe_5C(CO)_{17}]^{2-}$	26.2 ^5E (C_1)	23.2 *E (C_1)
IX	red $[Ir_6(CO)_{16}]$	15.9 ^5D (T_d)	
X	black $[Ir_6(CO)_{16}]$	22.7 ^5D (D_{2d})	17.3 *D (D_{2d})
XI	$[Rh_2Fe_4B(CO)_{16}]^-$	18.0 ^5D (D_{2d})	17.3 *D (D_{2d})
XII	$[M_6(CO)_{16}]$	22.0 ^5D (C_2)	21.0 *D (C_2)
XIII	$[Ru_6C(CO)_{16}][NEt_4]_2$	20.5 ^5D (C_s)	18.2 *D (C_s)
XIV	$[Fe_4CoRhC(CO)_{16}]$	18.5 ^5D (C_2)	
XV	$[M_6(CO)_{16}]$	20.1 ^5D (C_3)	
XVI	$[Fe_6C(CO)_{15}(NO)]$	20.8 ^5D (C_1)	20.5 *D (C_1)
XVII	$[Ru_6C(CO)_{14}(NO)_2]$	25.6 ^5D (C_2)	21.0 *D (C_2)
XVIII	$[Ir_6(CO)_{15}]^{2-}$	20.2 ^5B (D_3)	
XIX	$[M_6(CO)_{15}]$	24.0 ^5B (C_3)	
XX	$[Co_6(CO)_{15}]^{2-}$	23.5 ^5B (C_{3v})	
XXI	$[Fe_3Rh_3C(CO)_{15}]^-$	22.4 ^5B (C_{3v})	
XXII	$[Co_6H(CO)_{15}]^-$	26.7 ^5B (C_{2v})	20.1 *B (C_{2v})
XXIII	$[Fe_6C(CO)_{13}(NO)_2]^{2-}$	26.3 ^5B (C_2)	22.4 *B (C_2)
XXIV	$[Rh_5Pt(CO)_{15}]^-$	22.2 ^5B (C_{2v})	21.8 *B (C_{2v})
XXV	$[Co_6(CO)_{14}]^{4-}$	24.1 ^5A (D_{3d})	
XXVI	$[M_6(CO)_{14}]$	19.4 ^5A (D_{3d})	
XXVII	$[Co_6C(CO)_{14}]^-$	28.6 ^5A (C_{2v})	24.6 *A (C_{2v})
XXVIII	$[Co_6C(CO)_{13}]^{2-}$	16.0 ^5A (C_2)	14.2 *A (C_2)
XXIX	$[Co_2Rh_4C(CO)_{13}]^{2-}$	22.2 ^5A (C_2)	18.4 *A (C_2)
XXX	$[Rh_6C(CO)_{13}]^{2-}$	23.6 ^5A (C_s)	19.4 *A (C_s)
XXXI	$[Co_6N(CO)_{13}]^-$	15.2 ^5A (C_s)	
XXXII	$[M_6(CO)_{13}]$	17.0 ^5A (C_s)	
XXXIII	$[Ni_6(CO)_{12}]^{2-}$	8.0 ^5A (D_{3d})	
XXXIV	$[M_6(CO)_{12}]$	4.1 ^5A (D_{3d})	
XXXV	$[M_6(CO)_{12}]$	34.0 ^5A (O_h)	

[a] Steric energies (kcal mol^{-1}) addressed using structure number, minimization conditions, parameter set, and symmetry label. A known example, if existent, is also reported. Key: (s) all the bridging carbonyl ligands have been constrained to be symmetric; (*) the carbonyl ligands have been left to asymmetrize and float over the EPS; (m) when the metal cage is distorted along the $O_h \rightarrow D_3$ coordinate, the energy drops to 28.9 kcal mol^{-1}. A–G refer to the parameter set used in the computation (see Table I).

Computational Results

Many different stereoisomers have been generated for BCMCs with stoichiometries ranging from $M_6(CO)_{12}$ to $M_6(CO)_{20}$; their connectivity patterns are graphically reported in Chart I (structures I–XXXV), where μ_2- and μ_3-bridging carbonyl ligands are represented by black bonds and dotted faces, respectively, while the number of terminal CO ligands, belonging to each metal center, is written inside the atom circles. Each stereoisomer is addressed in the text by the structure number, its overall symmetry (two species can have the same connectivity but different symmetry), and the labels specifying the computational details and the cluster size (vide infra). The steric potential energy (E_s) for all the different stereogeometries has been minimized, and the results are summarized in Table II.[39] The computations were performed with several parameter sets (A–G), differing mainly in the metal covalent radius, to mimic small and large metal cluster polyhedra with metal–metal bond lengths ranging from 2.50 to 3.00 Å. The geometries were optimized by either imposing a "fixed" connectivity on the carbonyl ligands (superscript s) or allowing them to float over the EPS until they reached the closest available minimum (asterisk).[40]

(39) Few nitrosyl derivatives (NO is considered here as "isosteric" with CO) and mixed-metal clusters are included in the table. This allows the experimental observation of moderately "high-energy" ligand stereogeometries. In fact, differences in the ligand donor abilities, like those in metal electron requirements, can stabilize uneven ligand distributions on the cluster surface.

Table III[a]

	b	M_1–C	M_2–C	M_3–C	b	M_1–C′	M_2–C′
$[Ru_6(CO)_{18}]^{2-}$	2	2.06	2.23	2.51	2	2.03	2.15
V *E (C_2)	2	1.99	2.04	2.61	2	1.93	2.14
$[MoFe_5C(CO)_{17}]^{2-}$	1	1.88	2.05		1	1.84	2.41
VIII *E (C_1)	1	1.96	2.06		1	1.86	2.50
black $[Ir_6(CO)_{16}]$	4	1.99	2.25				
$[Ru_6C(CO)_{16}][AsPh_4]_2$	4	2.03	2.21				
$[RhFe_5C(CO)_{16}]^-$	4	1.86	2.57				
X *D (D_{2d}) = XI *D (D_{2d})	4	1.84	2.56				
$[Ru_6C(CO)_{16}][NEt_4]_2$	3	1.97	2.23		1	1.79	2.61
$[Fe_6C(CO)_{16}]^{2-}$	3	1.76	2.18		1	1.55	2.65
XIII *D (C_s)	3	1.89	2.18		1	1.82	2.85
$[Fe_4CoRhC(CO)_{16}]$	2	1.96	2.24				
XIV *D (C_2)	2	1.98	1.98				
$[Fe_6C(CO)_{15}(NO)]$	2	1.97	2.06				
XVI *D (C_1)	2	1.92	2.06				
$[Ru_6C(CO)_{14}(NO)_2]$	4	2.04	2.23				
XVII *D (C_2) = XII *D (C_2)	4	1.85	2.43				
$[Co_6H(CO)_{15}]^-$	4	1.83	2.19				
XXII *B (C_{2v})	4	1.76	2.48				
$[Fe_6C(CO)_{13}(NO)_2]^{2-}$	2	1.82	2.56				
XXIII *B (C_2)	2	1.76	2.57				
$[Rh_5Pt(CO)_{15}]^-$	2	2.13	2.22	2.22			
XXIV *B (C_{2v})	2	1.97	2.10	2.10			
$[Co_6C(CO)_{14}]^-$	6	1.85	2.05				
XXVII *A (C_{2v})	6	1.75	2.08				
$[Co_6C(CO)_{13}]^{2-}$	4	1.89	1.98				
XXVIII *A (C_2)	4	1.75	2.10				
$[Co_2Rh_4C(CO)_{13}]^{2-}$	2	1.92	2.09				
XXIX *A (C_2)	4	1.74	2.11				
$[Rh_6C(CO)_{13}]^{2-}$	2	1.92	2.35				
XXX *A (C_s)	2	1.72	2.33				

[a] Comparison between observed and calculated local geometries of semibridging carbonyl ligands. Calculated geometries are addressed throughout using structure number, parameter set, and symmetry label. Asterisks indicate that all carbonyl ligands have been left to asymmetrize and float over the EPS. [b] Number of equivalent asymmetric carbonyl ligands (μ_2 or μ_3).

A comparison between observed and calculated geometries for the semibridging carbonyl ligands is reported in Table III. The absolute agreement is less than satisfactory because the systematic neglect of many important interactions (see below); nevertheless, distortions are always anticipated in the correct direction. The computed energies have little meaning outside the context of the present paper and should be used only to compare different conformers. This is not a serious limitation because the term "conformer", within the EPS formalism, is comprehensive also of all the stereoisomers which, differing in the metal–carbonyl connectivity, would normally be considered "constitutional isomers".

The steric potential energy per carbonyl group ($E_{CO} = E_s/n_{CO}$) can be used to compare roughly the different stoichiometries and, using the E_{CO} of octahedral mononuclear complexes $M(CO)_6$ as a reference (E_{CO} = 3.6 and 1.7 kcal mol^{-1} carbonyl^{-1} for M–C = 1.80 and 1.95 Å, respectively), to foresee the intrinsic steric stability of a selected isomer.[41] However, care must be taken in this sort of comparison: a mononuclear complex can easily resist a steric strain of 3.6 kcal mol^{-1} carbonyl^{-1} because of the "strong" M–C bonds, while the "weaker" M–M bonds might not guarantee the same stability for a cluster.

The major contribution to the computed steric energies arises from the nonbonding interactions. The valence forces maintain

(40) For instance, when the local-connectivity assumption is made, $M_6(\mu_3\text{-CO})_4(\mu_2\text{-CO})_{12}$ (a high-energy stereoisomer which can be "obtained" imposing the proper metal-to-carbonyl connectivity) relaxes to $M_6(\mu_3\text{-CO})_4(CO)_{12}$ (IX), the lowest energy stereoisomer of $M_6(CO)_{16}$; while $M_6(\mu_2\text{-CO})_4(CO)_{12}$ (X) relaxes to $M_6(CO)_{16}$ (XI), which lies in a local minimum of the "steric" PES.

(41) Lauher, for instance, has considered "sterically allowed" $Mn_4(CO)_{16}$ (T_d), which, using a slightly different force field, has an E_{CO} (4.7 kcal mol^{-1} carbonyl^{-1}; M–M = 2.644 Å) close to that of an octahedral $M(CO)_6$ complex (E_{CO} = 4.0 kcal mol^{-1} carbonyl^{-1}; M–C = 1.80 Å).[22]

Chart I

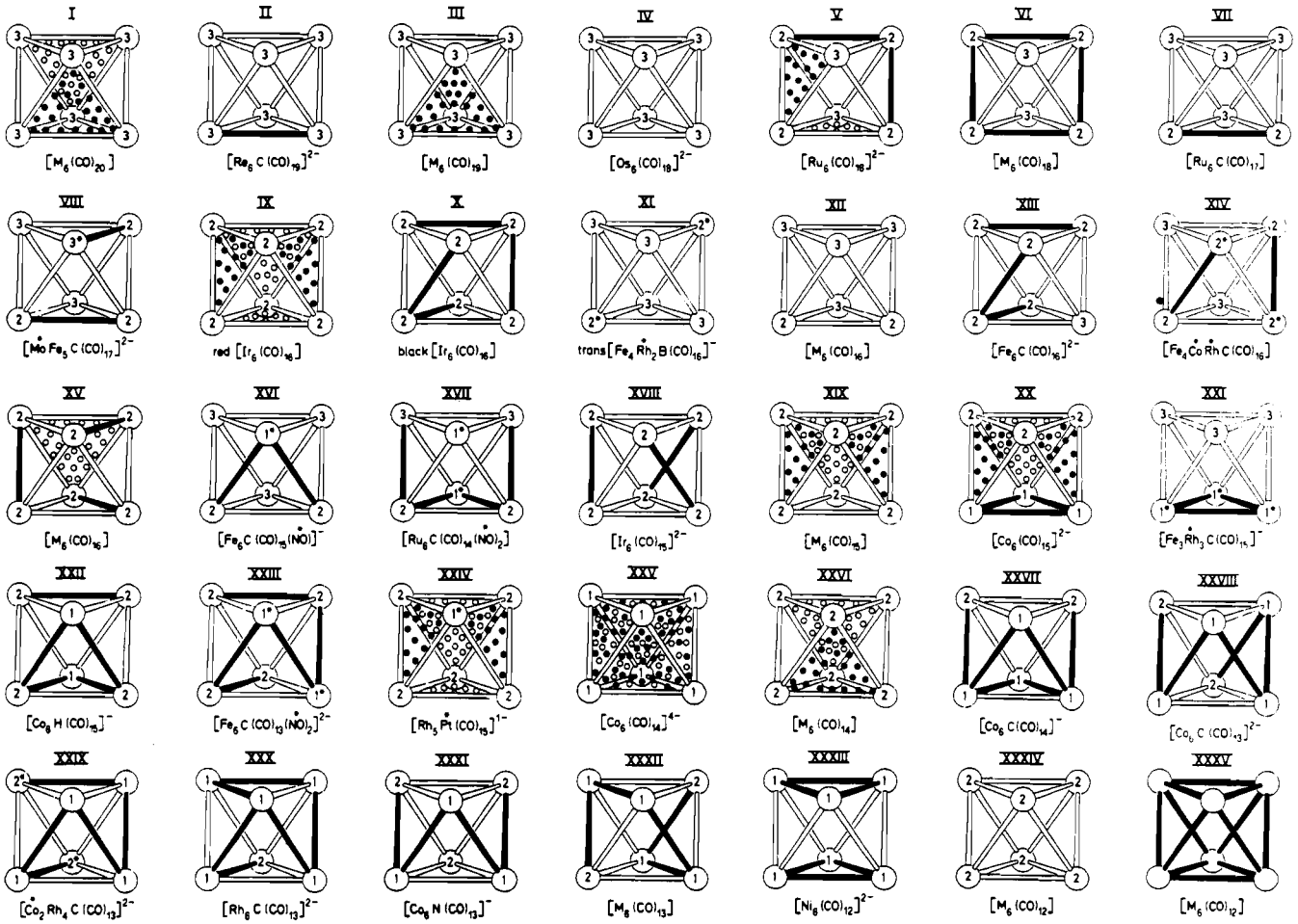

the carbonyl ligands on the EPS without a substantial contribution to the steric energy because of the lack of bending and torsional terms. Moreover, the globularity of many carbonyl clusters makes dipolar interactions rather insensitive to the carbonyls' geometry. *Hence, the program models a carbonyl cluster as if it were under the influence of the (intramolecular) vdW forces only* and the comparison between modeled and experimental structures should allow the recognition of the presence of other forces at work.

Discussion on Selected Examples

$[Re_6C(\mu_2\text{-}CO)(CO)_{18}]^{2-}$ (II (C_s))[7] could be considered the "most sterically crowded" octahedral BCMC;[42] nevertheless, it easily adds H^+, affording the even more crowded $[Re_6C(\mu_2\text{-}H)(\mu_2\text{-}CO)(CO)_{18}]^-$.[43] Moreover, if we consider $[Re(CO)_3]^+$ to be isolobal with CO and to have a similar steric hindrance, the stability of $[Re_6C(CO)_{18}(\mu_3\text{-}Re(CO)_3)_2]^{2-}$[44] leads us to consider the possible existence of the (not yet characterized) compound $[Re_6C(CO)_{20}]$. The present computations (parameter set G) show that $M_6(\mu_3\text{-}CO)_2(CO)_{18}$ (I (C_{3v})) is not particularly crowded, having a reasonable E_{CO} (1.6 kcal mol^{-1} carbonyl^{-1}) when compared to that of an octahedral mononuclear complex. Nevertheless, steric allowance does not imply the presence of a minimum in the "true" PES nor the existence of a kinetically allowed chemical path affording a desired species, since MM gives no account of the electronic or valence forces acting on a specific compound.

A feature common to most of the BCMCs is the presence of a large spread of the metal–metal bond distances, often attributed to intra- or intermolecular steric effects.[45] Assigning different reference values to different polyhedral edges, i.e. setting the energy required for the deformation of the metal cage to zero, it is possible to study the relative ligand crowding of differently distorted metal cages. For instance, the commonly observed $O_h \rightarrow D_3$ distortion leads to a ligand steric energy relief of only 2.3 kcal mol^{-1} when alternated interbasal edges of IV are lengthened from 2.80 to 3.00 Å (corresponding to a relative rotation of the basal triangles of 12°). This is a rather low energy if compared to that computed using the parameters of Table I for a 0.2-Å stretching of three M–M bonds (11.1 kcal mol^{-1}). A better parametrization of the metal–metal interaction and a full discussion of the metal cluster distortion are beyond the scope of this paper, but unless a smaller force constant and/or a larger cubic stretch term (anharmonicity constant) are/is used for the M–M interactions, the intramolecular steric forces alone cannot account for the observed polyhedral distortions.

The most stable (and common) ligand arrangement for 16 CO's is that of $[Rh_6(CO)_{16}]$ (IX (T_d)).[46] $[Ir_6(CO)_{16}]$ is polymorphic

(42) The carbonyl-to-metal ratio is not a good indicator for the steric crowding and should be weighted to account for differences in the metal–metal bond lengths and in the metal cluster shape. Mingos, D. P. M. *Inorg. Chem.* **1982**, *21*, 466. Generalizing the Tolman cone angle concept, Mingos has proposed those of "cluster" and "$M(CO)_n$" cone angles. This is an empirical way to account for variance in the shape and dimensions of the metal cluster, and a maximum number of 18 carbonyl ligands was deduced for an octahedron of edge 2.90 Å.

(43) In many cases, MM cannot discriminate between different alternatives; nevertheless once the "correct" stereochemistry is assumed, the experimental and modeled stereogeometries are surprisingly similar. II-C_s/III-C_3 and $[Re_6C(\mu_2\text{-}CO)(CO)_{18}]^{2-}$;[7] IV/V* and $[M_6(CO)_{18}]^{2-}$ (M = Ru): Jackson, P. F.; Johnson, B. F. G.; Lewis, J.; McPartlin, M.; Nelson, W. J. H. *J. Chem. Soc., Chem. Commun.* **1979**, 735. IV/V* and $[M_6(CO)_{18}]^{2-}$ (M = Os): McPartlin, M.; Eady, C. R.; Johnson, B. F. G.; Lewis, J. *J. Chem. Soc., Chem. Commun.* **1976**, 883.

(44) Ciani, G.; D'Alfonso, G.; Freni, M.; Romiti, P.; Sironi, A. *J. Chem. Soc., Chem. Commun.* **1982**, 705.

(45) Albano, V. G.; Braga, D. In *Accurate Molecular Structures*; Domenicano, A., Hargittai, I., Eds.; Oxford University Press: Oxford, U.K., 1991.

(46) Corey, E. R.; Dahl, L. F.; Beck, W. *J. Am. Chem. Soc.* **1963**, *85*, 1202.

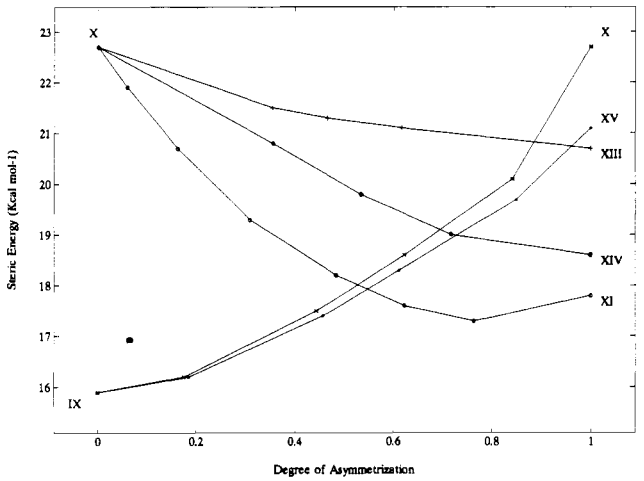

Figure 5. Energetics of some selected isomeric interconversions of the $M_6(CO)_{16}$ clusters. The reaction coordinate is the degree of asymmetry of the pertinent bridging CO's, $(D_{long} - D_{short})/(D_{max} - D_{min})$. The processes involve the concerted motion of all the ligands, as expected for low-energy transformations: (○) $X(D_{2d}) \rightarrow XI(D_{2d})$ $\mu_2 \rightarrow \mu_1$ interconversion of four CO's along a D_{2d} path; (+) $X(C_{2v}) \rightarrow XIII(C_s)$ $\mu_2 \rightarrow \mu_1$ interconversion of one CO along a C_s path [when the four μ_2-CO's are symmetric, $X(C_{2v})$, in spite of the different symmetry label, is rather similar to $X(D_{2d})$ and has the same E_s]; (●) $X(C_{2v}) \rightarrow XIV(C_2)$ $\mu_2 \rightarrow \mu_1$ interconversion of two CO's along a C_2 path; (×) $IX(T_d) \rightarrow X(D_{2d})$ $\mu_3 \rightarrow \mu_2$ interconversion of four CO's along a D_{2d} path; (✱) $IX(T_d) \rightarrow XV(C_3)$ $\mu_3 \rightarrow \mu_2$ interconversion of three CO's along a C_3 path.

and shows ligand isomerism in the solid state: in the *red* phase it is isomorphous with $[Rh_6(CO)_{16}]$ while, in the *black* one, it has the X (D_{2d}) stereogeometry, where the four μ_3-CO's of IX are transformed into four μ_2-CO's.[47] The crowd around the two most connected metals makes X unstable with respect to both the $\mu_2 \rightarrow \mu_3$ (X → IX) and the $\mu_2 \rightarrow$ terminal (X → XI) transformations (Figure 5). The present computations totally overlook the intermolecular interactions and the valence electron transfer coupled to the terminal–bridging CO transformation. For this reason, steric energies are better used to justify small distortions around a given geometry rather than to foresee the correct stereoisomer.[43] Thus, the more efficient packing of the black phase,[48] allows the detection of the "unfavorable" conformation X, which also gains some extra stability by an incipient X → XI transformation (the four μ_2-CO's are asymmetric). The X → XI transformation is nevertheless antagonized in $[Ir_6(CO)_{16}]$ by the need for a uniform local distribution of the valence electrons, and as a consequence, the black $[Ir_6(CO)_{16}]$ isomer is only slightly distorted; on the contrary, the $[RhFe_5C(CO)_{16}]^-$ and the *trans*-$[Rh_2Fe_4B(CO)_{16}]^-$ anions,[49,50] where the presence of a net charge and different metal atoms ensures a reasonable valence electron distribution, reach the minimum (steric) energy conformation, which is close to XI.[51]

$[Fe_4CoRhC(CO)_{16}]$ (XIV (C_2))[52] has two markedly asymmetric μ_2-CO's but the "steric" PES has a local minimum for symmetric μ_2-CO's. This suggests an electronic origin of the distortion and, consequently, a different rationalization of the crystal structure.[53] In fact, if the two-electron-richer metal atoms (Co and Rh) were in the two cis positions concerned with the long M–(μ_2-C) interactions, the carbonyls' asymmetry would be easily understandable on the basis of charge delocalization.

It is well-known that (i) there is a more widespread occurrence of bridging carbonysl in clusters of the lighter transition metals and (ii) μ_3-CO are (slightly) less common than μ_2-CO ligands in clusters of the heavier transition metals. This behavior can be related, as proposed by Evans, to the different sizes and energies of the d orbitals in the three transition series.[54] As a matter of fact, the low-energy $[M_6(CO)_{15}]$ isomer (XVIII) is observed in $[Ir_6(CO)_{15}]^{2-}$, while the smaller complexes $[Co_6(CO)_{15}]^{2-}$ and $[Co_6(\mu_6\text{-}H)(CO)_{15}]^-$ display the sterically less stable stereogeometries XX and XXII, which maximize the number of bridging CO's.[55] Analogously the larger $Ir_4(CO)_{12}$ assumes the lower energy T_d (or perhaps T) structure with only terminal CO's, while the smaller $Co_4(CO)_{12}$ prefers the (sterically) unfavorable C_{3v} structure with three μ_2-CO ligands.

Assuming that the relative stability of the CO polyhedra can be inspected by simple geometrical considerations and, later, by the use of a repulsive potential acting between the oxygen atoms alone, Johnson and Benfield argued that the number and the distribution of bridging and terminal CO groups in cluster carbonyls $M_m(CO)_n$ are determined by purely steric factors and reflect (i) the polyhedral arrangement of the n CO ligands and (ii) the orientation of the M_m unit within this polyhedron.[21] The need for a good fit between the ligand and the metal polyhedra and the idea that CO's pack into the space so as to minimize nonbonded interactions are also appealing and central to the present computations. Nevertheless the point on a sphere model (used to order in energy the multitude of possible oxygen polyhedra) is rather an oversimplification, since (with the usual MM atom pair potentials) the O···O interactions are hardly repulsive and the oxygen polyhedron alone does not mimic the $(CO)_n$ moiety sufficiently well. As a matter of fact, in the case of 14 CO's, XXV is the best solution to the fit of a metal octahedron and an oxygen polyhedron, but the most stable stereogeometry is (by far) XXVI, which has a rather unfavorable (bicapped hexagonal prismatic) oxygen envelope.[56] A further weakness of Johnson and Benfield's model arises from the fact that terminal and bridging carbonyl ligands have, intrinsically, different distances from the cluster center (B), the B···O distances being larger for the terminal CO's. The problem appears, for instance, in the $M_6(CO)_{12}$ case, where XXXIV (12 terminal CO's, B···O distance 4.11 Å) has the lowest steric energy while XXXV (12 μ_2-CO's, B···O distance 3.79 Å) has an amazingly high steric energy. Thus XXXV, in spite of

(47) Interconversion of the two isomers in solution was not detected; i.e., the IR spectra of the two isomers were different. Nevertheless, the two phases are so insoluble that perhaps IR spectrum refers to "a suspension of fine powders" rather than to a solution (Garlaschelli, L. Personal communication).
(48) Braga, D.; Grepioni, F. *Acta Crystallogr.* **1989**, *B45*, 378.
(49) Slovokhotov, Y. L.; Struchkov, Y. T.; Lopatin, V. E.; Gubin, S. P. *J. Organomet. Chem.* **1984**, *266*, 139.
(50) The *trans*-$[Rh_2Fe_4B(CO)_{16}]^-$ anion is described in the original paper as having four semibridging CO's even if the reported ORTEP diagram showed only terminal CO's: Khattar, R.; Puga, J.; Fehlner, T. P.; Rheingold, A. L. *J. Am. Chem. Soc.* **1989**, *111*, 1877.
(51) Note that the stability of XI is due to the slight bending of the (former μ_2) CO's toward the two "ligand-deficient" metal atoms; this is less effective in the cis isomer XII, which consequently has higher energy. The preparation of *trans*-$[Rh_2Fe_4B(CO)_{16}]^-$ proceeds through the cis isomer, which slowly transforms into the most stable trans isomer: Bandyopadhyay, A. K.; Khattar, R.; Fehlner, T. P. *Inorg. Chem.* **1989**, *28*, 4434.
(52) Lopatin, V. E.; Gubin, S. P.; Mikova, N. M.; Tsybenov, M. T.; Slovokhotov, Y. L.; Struchkov, Y. T. *J. Organomet. Chem.* **1985**, *292*, 275.
(53) The original model proposed a Rh/Fe disorder over the cis M_1/M_2 positions and a Co/Fe disorder over the trans M_3/M_5 ones (M_1, M_2, M_3, and M_5 being the metal atoms concerned with μ_2-CO's). In a conventional X-ray diffraction experiment, Co and Fe are not distinguishable; therefore, the proposed model (Rh/Co disordered over the cis M_1/M_2 positions) explains the observed fractional occupancies of Rh in M_1 and M_2 as well but, in addition, justifies the observed distortions.
(54) Evans, D. G. *J. Chem. Soc., Chem. Commun.* **1983**, 675. As the more contracted 3d orbitals transform into the less contracted 5d orbitals, the π overlap becomes more effective; this stabilizes the terminal over the bridging carbonyl because the (metal)t_{2g}–π^*(carbonyls) interactions, which are responsible for the M → CO back-donation, arise from π overlap in the case of terminal but from σ overlap in the case of bridging carbonyls.
(55) (a) M = Co: Albano, V.; Chini, P.; Scatturin, V. *J. Chem. Soc., Chem. Commun.* **1968**, 163. (b) Hart, D. W.; Teller, R. G.; Wei, C. Y.; Bau, R.; Longoni, G.; Campanella, S.; Chini, P.; Koetzle, T. F. *J. Am. Chem. Soc.* **1981**, *103*, 1458. (c) M = Ir: Demartin, F.; Manassero, M.; Sansoni, M.; Garlaschelli, L.; Martinengo, S.; Canziani, F. *J. Chem. Soc., Chem. Commun.* **1980**, 903.
(56) The best 14-vertex polyhedra were the bicapped hexagonal antiprism (BHA), the omnicapped cube (OC), and others more complex. The bicapped hexagonal prism was not included among the first six stable polyhedra. The use of the most stable BHA was suggested to imply a severe trigonal distortion of the metal polyhedron; thus the best suggested solution was to align the 4-fold axis of the OC with that of the metal octahedron.[21]

having a better shaped oxygen polyhedron than XXXIV (cuboctahedral versus a irregularly folded cuboctahedral shape),[57] has a larger steric energy because its oxygen polyhedron is smaller than that of XXXIV. There is in fact a rough inverse correlation between steric energies and cluster volumes because, as long as the numbers of carbonyl ligands are the same, smaller clusters must have shorter (repulsive) C···C interactions.

Thirteen ligands are difficult to arrange reasonably around a metal octahedron; ligand compactness conflicts with electronic homogeneity, as demonstrated by the careful structural comparison of the isoelectronic, but not isostructural, $[Co_6C(CO)_{13}]^{2-}$ (XXVIII (C_2)),[58] $[Co_2Rh_4C(CO)_{13}]^{2-}$ (XXIX (C_2)),[59] and $[Rh_6C(CO)_{13}]^{2-}$ (XXX (C_s))[60] species. The present computations confirm the proposed order (XXVIII < XXIX < XXX) for the steric crowding in the three carbido compounds[59] and substantiate the interplay, as the metal cage becomes larger, between steric and electronic factors in dominating the conformational choice.[61] Nevertheless, computer simulations poorly reproduce the nearly planar conformation of the $M(CO)(\mu_2\text{-}CO)_2$ moieties, the *radial* nature of many terminal CO's, and the "holes" found in $[Co_2Rh_4C(CO)_{13}]^{2-}$ and $[Rh_6C(CO)_{13}]^{2-}$ ligand arrangements, confirming that some electronic factors are at work. In fact, when the local stereochemistry is controlled by the 1,3 interactions only, the CO ligands always prefer to equalize the local steric crowding and to occupy all the space available around the metal cage, rather than assume a local or global stereogeometry fulfilling some electronic requirement.[62]

Conclusions

In the present approach, emphasis has been placed on intramolecular steric interactions which are thought to be the only factor affecting carbonyl ligands in the choice for their *local coordination geometry*. In other words, the structures of metal carbonyls have been modeled as being determined by the packing of ligands around the surface of the metal core, rather than as being determined by the sum of the structures about the individual metal atoms. This is cleary an oversimplification: (i) although there is no reason to attribute a larger stability to bridging carbonyl ligands than to terminal ones, and the few available thermochemical data support the idea of similar binding energies for the three coordination modes,[63] bridging and terminal CO's have different π-acidities and hence have different effects on the adjacent metals (the greater the electron density on the metals, the larger the number of bridging carbonyls);[64] (ii) equidistribution of the volume around the individual metal centers does not always imply an analogous equidistribution of the valence electrons and a good equalization of the charges; (iii) there is a more widespread occurrence of bridging carbonyls in clusters of the lighter transition metals (with respect to those of the second and third rows);[54] (iv) local ligand stereogeometry is often suggested by the inert-gas rule for the metal vertex; (v) some metals present a clear anisotropy in their local ligand stereogeometry (for instance Pt often has strong (short) in-plane and weak (long) out-of-plane interactions). Most of the structural information on metal carbonyl clusters arises from solid-state structures where the conformations are strongly affected, in a rather unpredictable way, by the presence of the crystal lattice. This fact complicates the comparison between experimental and modeled stereogeometries. Nevertheless, such comparison has clearly shown that "real" structures are only occasionally found in the global minimum of the "steric" PES; more frequently they are close to a local minimum if not somewhere along the valley connecting a minimum to a saddle point. Thus *intramolecular steric interactions do not appear to be the leading term in determining BCMC stereogeometries in the solid state*. It is only the interplay among many different factors (inter- and intramolecular steric interactions, charge and local bookkeeping equalization, and more specific electronic effects) that determines the real structure. Therefore *steric energies are properly used only to justify small distortions around a given geometry or to exclude a particularly crowded stereoisomer rather than to foresee the correct one*.

The program is a powerful modeler of carbonyl metal clusters (symmetry constraints can be imposed and each internal coordinate can be set at any required value) and either can be used to directly sample the "steric" PES or can be used as a *source of sterically reasonable geometries* for quantum mechanical computations. The program allows the contemporary presence of "locally connected" and "normal" atoms; therefore, clusters with ligands other than CO might be straightforwardly considered, provided that a reasonable force field has been developed. Moreover, the local connectivity approach can be extended, in principle, to all the ligands showing a large coordinative versatility and tendency to a fluxional behavior (for instance H^-).[65]

Acknowledgment. I am indebted to G. Ciani, G. D'Alfonso, N. Masciocchi, M. Moret, H. Molinari, and D. Proserpio, who carefully read the manuscript, suggesting corrections and solutions to many problems. The reviewers' stimulating suggestions helped in clarifying the text.

Supplementary Material Available: Figure S1, showing a plot of eq 2, Figure S2, showing a plot of the EPS shape within a triangle, Table S1, giving selected structural information on the known octahedral carbonyl and nitrosyl clusters, and ORTEP plots and lists of relevant bonding parameters for the 14 computed stereogeometries reported in Table III (33 pages). Ordering information is given on any current masthead page.

(57) The best 12-vertex polyhedra, in Johnson and Benfield's model, are the icosahedron, the cuboctahedron, and the anticuboctahedron.[21]

(58) Albano, V. G.; Braga, D.; Martinengo, S. *J. Chem. Soc., Dalton Trans.* **1986**, 981.

(59) Albano, V. G.; Braga, D.; Grepioni, F.; Della Pergola, R.; Garlaschelli, L.; Fumagalli, A. *J. Chem. Soc., Dalton Trans.* **1989**, 879.

(60) Albano, V. G.; Braga, D.; Martinengo, S. *J. Chem. Soc., Dalton Trans.* **1981**, 717.

(61) The presence of an interstitial carbide causes such a large distortion in the metal backbone (because of the intrinsically small octahedral hole) that a more realistic evaluation of the steric crowding should be made using experimental cluster dimensions rather than almost regular octahedra. When the "true" M–M bond distances are introduced and the CO's are modeled by the parameter set B of Table I, the new steric energies (9.5, 12.6, and 12.2 kcal mol^{-1} for XXVIII, XXIX, and XXX, respectively) confirm that XXVIII is the least hindered stereoisomer but the energy order for XXIX and XXX is reversed. XXVIII is reasonably similar to $[Co_6C(CO)_{13}]^{2-}$, whose stereochemistry is assumed to be under the control of steric factors.[59]

(62) In the case of $[Co_2Rh_4C(CO)_{13}]^{2-}$, the lengthening of the unbridged metal–metal interactions on two opposite metals (due to the steric needs of the interstitial carbide) affords two almost square-planar Rh atoms whose local electron bookkeeping is close to 16 valence electrons (because of the lengthening of the M–M bonds). Thus, the equatorial ligand folding, even if it releases steric energy, is antagonized by the usual electronic factors which stabilize 16-valence-electron square-planar Rh complexes.

(63) Connor, J. A. In *Transition Metal Clusters*; Johnson, B. F. G., Ed.; Wiley: New York, 1980; p 345.

(64) Chini, P.; Longoni, G.; Albano, V. G. *Adv. Organomet. Chem.* **1976**, *14*, 285.

(65) Ligand mobility of chemisorbed molecules on metal surfaces is an important requirement for heterogeneous catalysis; in the light of the suggested analogy between metal clusters and chemisorbed states on metal surfaces (Muetterties, E. L.; Rhodin, T. N.; Band, E.; Brucker, C. F.; Pretzer, W. R. *Chem. Rev.* **1979**, *79*, 91), it seems appealing to envisage a possible use of the local connectivity methodology in the study of ligand-covered flat metal surfaces which, lacking structural analogues in the discrete metal cluster family, need to be theoretically modeled.